MATCH
Communications in Mathematical and in Computer Chemistry

MATCH Commun. Math. Comput. Chem. **88** (2022) 437-460
ISSN: 0340-6253
doi: 10.46793/match.88-2.437N

Mathematical Investigations of a Kinetic Model for Glycerol Hydrogenolysis Via Heterogeneous Catalysis

Thandokuhle Quinton Ndlovu[1], **Mzamo L. Shozi**[2], **Fernando P. da Costa**[3]

[1] *African Institute for Mathematical Sciences, South Africa*
ndlovuquinton4@gmail.com

[2] *University of KwaZulu-Natal, South Africa*
Shozim2@ukzn.ac.za

[3] *Universidade Aberta and Centre for Mathematical Analysis, Geometry and Dynamical Systems, Portugal*
Fernando.Costa@uab.pt

(Received October 13, 2021)

Abstract

In this paper we report on some mathematical investigations of the chemical process for the hydrogenolysis of glycerol over a heterogeneous metal catalyst. The main interest of this process is related to the fact that glycerol is produced as a by-product in the production of biodiesel in huge amounts that are expected to exceed the projected demands. This makes the sustainability of biodiesel production depend on the conversion of the glycerol into useful products hence it is a desirable goal to have effective conversion methods. A reaction model from literature is used to derive a system of ordinary differential equations (ODE) which is then analysed using methods from qualitative analysis of ODEs. Numerical solutions of the system are simulated to try and find out the solution's behaviour in the chemistry point of view. It was found that all solutions of the model converge to some stable limit point in a 2-dimensional plane in the positive cone of the $\mathbb{R}^5$ phase space, and the limit point depends on the values of rate constants k_i as well as on the hydrogen to glycerol initial ratios. Even though the results are based on a specific kinetic model, it is hoped that they may help in providing tools for better understanding and description of the reaction.

1 Introduction

The effects that climate change has on the environment cannot go unnoticed and as a result, has attracted researchers to find ways to ensure the situation remains controllable. Literature has shown that fossil fuels are one of the leading contributors to climate change due to their massive production of carbon dioxide, a gas reported to contribute massively to climate change [11]. There exists various approaches to minimize the destructions caused by climate change which includes the use of biodiesel. This is a biofuel which hopes to decrease the absolute dependence on crude oil, one of the major contributors to climate change [4].

According to Zhao et al. [18], during the production of biodiesel, another chemical called glycerol is produced in very large amounts and it is proposed that the production of glycerol will exceed its market demands in the near future. Glycerol has got a lot of applications as it is used in the food industry, pharmaceuticals etc. In some work reported by Torres et al. [16], it is stated that even though the production of biodiesel has been commercialized, the tenability of this process depends on the conversion of glycerol into its useful chemical derivatives. Therefore, there has been on-going research on how to convert the glycerol into suitable chemicals using different chemical methods and amongst those, hydrogenolysis is one of them. However in the work of Pandhare et al. [11], it is reported that not much research on the kinetics underlying these reactions has been done. As a result, in this study we seek to mathematically investigate the kinetics of a model for catalysed hydrogenolysis of glycerol using methods from the qualitative analysis of ODEs in an attempt to provide tools to describe and understand the reaction better. Numerical solutions to the model are simulated to try and understand the reaction's behaviour in the chemistry point of view as well as compare the model results to those obtained experimentally.

As steps towards this goal, we consider a reaction model in a report by Shozi et al. [14] for the hydrogenolysis of glycerol using Cu-Re/ZnO catalyst, from which we derive a system of ODEs that governs the reaction. From the mathematical model we;

- analyse it using techniques from qualitative analysis of ODEs,
- perform numerical simulations of the model to compare with the experimental re-

sults and investigate the factors that affects the reaction,

- derive some general result(s) from the analysis about the reaction.

2 Preliminaries

We first recall some existing kinetic models on the hydrogenolysis of glycerol. However, for us to understand the mathematics behind the models, we first need to understand the chemical background of the process that results in the production of glycerol and the general result on the reaction for glycerol hydrogenolysis. We first look at the summary of the biodiesel production process, which consequently leads to the production of glycerol.

2.1 Biodiesel production

Biodiesel is produced mainly from animal fats and vegetable oil through a process called transesterification [18]. Figure 1 illustrates an outline of the processes involved in the production of biodiesel.

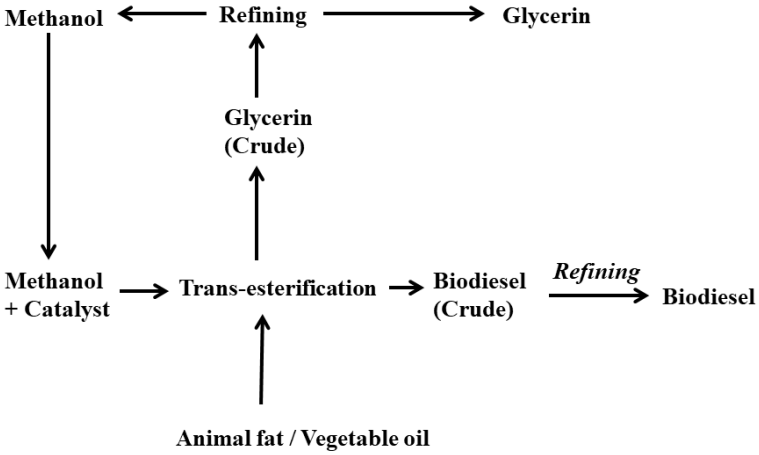

Figure 1. The biodiesel production process.

In Figure 1 it can be seen that glycerin, commonly called glycerol is also produced. According to Jin et al. [13], for every 10 kg of biodiesel produced, 1 kg of glycerol is also formed as a by-product. Likewise, Zhao et al. [18] reported that in 2016 the global

production of biodiesel was approximately 32.8 million tonnes along with 3.28 million tonnes of glycerol as a by-product. This means that the sustainability and viability of commercializing the production of biodiesel lies on the utilization of glycerol [16]. It is therefore expected that with the increase in the production of biodiesel, more glycerol will be produced up to a point where the market cannot accommodate the excess. Lahr and Shanks [8] projects that by the year 2020, the production of glycerol will be 6 times more than the market demand. This is a cause for concern. As a result, studies on how to convert the glycerol into usable end products are of great interest [15].

The physical and chemical properties of glycerol allows it to be used in numerous industrial applications [17]. It has, therefore a variety of chemical applications, such as a blend in gasoline, coating in polymers, cosmetics, solvents, detergents, sweeteners and so on. Researchers have been involved in studies on how the glycerol can be converted effectively into its useful chemical derivatives. There are numerous methods used to convert glycerol into other useful chemicals, and this includes the use of catalysts alongside the accompanying reaction of interest such as etherification, esterification, fermentation, dehydration, hydrogenolysis etc, depending on the desired chemical products [2]. For the purposes of this study, we focused on the hydrogenolysis reaction, which is briefly described in the next section.

2.2 General results on hydrogenolysis of glycerol

The hydrogenolysis of glycerol is a chemical reaction that involves the cleaving of chemical bonds of glycerol by hydrogen in the presence of a metal catalyst [2] leadings to the production of 1,2-propanediol (1,2-PD), 1,3-propanediol (1,3-PD) and ethlyene glycol (EG) as main products, as well as other secondary products, such as ethanol, propanol and methane, depending on the catalyst used [15]. The main products have a large number of industrial applications such as being used as coolants, in manufacturing of fibre glass, in cosmetics, as well as in ink production [18]. A general reaction scheme for the possible products of catalytic glycerol hydrogenolysis is shown in Figure 2.

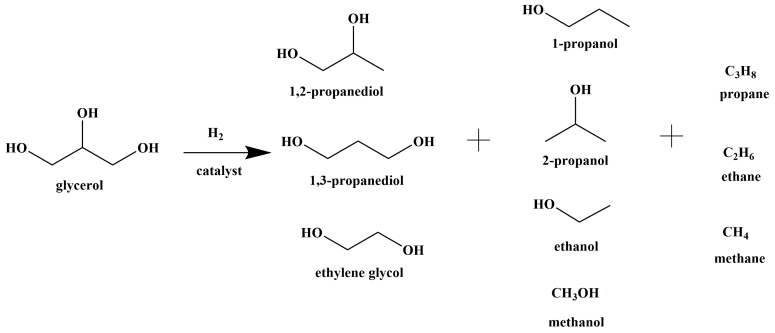

Figure 2. Main products from hydrogenolysis of glycerol; Wang et al. [17]

We have looked at the chemical background of the entire process that leads to the production of glycerol. We next present the chemical problem and the mathematical model to be studied.

3 The chemical problem, mathematical model and its basic properties

In this section we discuss the chemical problem in terms of its reaction mechanism and the experimental results, then formulate the mathematical model using ordinary differential equations. We use a scheme by Shozi et al. [14] to formulate the model since we have the experimental data that accompanies the scheme, making it possible to compare the model simulations with experimental results as well as estimate the reaction parameters. We start with a brief summary of the reaction, focusing mainly on the mechanism and the experimental results.

3.1 Reaction mechanism

Chemists have reported on the different reactions that have been studied for the catalytic hydrogenolysis of glycerol, however for purposes of this study we consider one reaction reported by Shozi et al. [14]. This reaction involves the use of a Cu-Re/ZnO catalyst, hydrogen and glycerol as the main reactants and the reaction is carried at suitable temperatures, around 2500C and hydrogen pressure of 60 bar [14].

3.1.1 Adsorption

The reaction involves the use of a metal catalyst where glycerol and hydrogen get adsorbed on the catalyst's site. Then, the adsorbed species react forming the products while regenerating the catalyst [11].

3.1.2 Reaction scheme

Since the reaction results into a complex network of parallel reactions, different gaseous and liquid phase products are obtained. Shozi et al. [14] proposed a reaction mechanism for possible pathways of glycerol hydrogenolysis. The reaction proceeds through the initial formation of glyceraldehyde (G_e), glycolaldehyde (G_O) and formic acid (F) as intermediates through the removal of hydrogen from the glycerol. Further hydrogenolysis then gives the products, mainly ethylene glycol, methanol and carbon monoxide depending on the catalyst used. A scheme of the reaction network is presented in Figure 3.

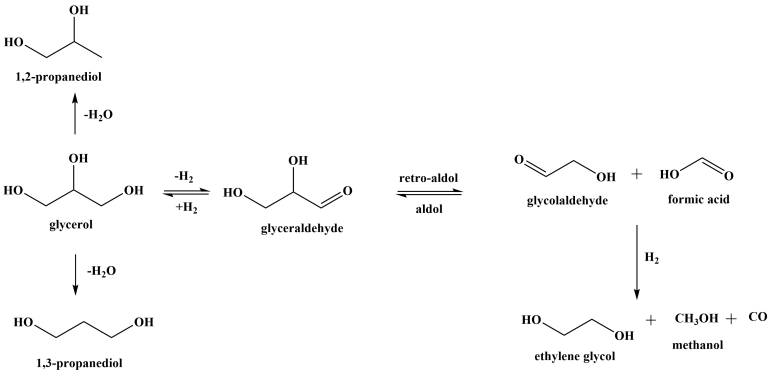

Figure 3. Reaction pathway for the conversion of glycerol over Cu/ZnO catalysts (Shozi et al. [14])

From the proposed mechanism, it is believed that retro-aldol conversion of glyceraldehyde is the main path for the formation of C_{1-2} molecules such as EG and methanol. Also, the formed 1,2-PD can be decomposed further into EG using suitable experimental conditions. At the end of the reaction they had 2 layers; an aqueous and an organic layer. The organic layer was analysed for products using gas chromatography (GC). The gases collected were also analysed using GC instruments and concentrations of products were determined and recorded.

However, due the Cu-Re/ZnO catalyst used in the experiment of Shozi et al. [14], it was reported that the 1,3-PD and the carbon monoxide were produced in very small amounts compared to the EG and 1,2-PD, and the methanol was around 25% of the EG. It was also reported that increasing the amount of hydrogen results in an increase in the production of EG over 1,2-PD. In a similar way, decreasing the amount of hydrogen resulted in a decrease in EG produced over 1,2-PD.

It must be noted that, from the reaction given by (1), it is seen that the rate of production of 1,3-PD could the same as that of 1,2-PD. However, experimentally this was not the case: with the Cu-Re/ZnO catalyst used in the experiment of Shozi et al. [14] it was reported that the 1,3-PD and the carbon monoxide were produced in very small amounts compared to the EG and 1,2-PD, and the methanol was around 25% of the EG. These evidence can point to some limitations of the model in [14]. It is believed that this is due to the fact that the true reaction scheme has a large number of side reactions and, as a consequence, getting the exact chemical model becomes a challenge.

3.2 Model development

To simplify the writing of the mathematical equations of the model, we introduce new notation for each of the species involved in the reaction presented in Table refParameters. In this notation we do not distinguish between 1,2-PD and 1,3-PD (as briefly discussed below the last one is reported to have been produced in very small amounts) and denote the their global concentratio by X_5; we also assume from the start that at the beginning of the process the concentrations of G_O and F are equal (they are, in fact, equal to zero) so that their amount at any later time will be equal and will be denoted by X_3.

Table 1. Simplified notation for the chemicals.

Old notation	New notation
G	X_1
G_e	X_2
$G_O = F$	X_3
EG	X_4
PD	X_5

With this notation and taking into consideration the discussion above a more compact

way of writing the chemical reactions network depicted in Fig 3 is the following

$$\mathrm{X}_5 \xleftarrow{k_0} \mathrm{X}_1 \underset{k_{-1}\ (+\mathrm{H}_2)}{\overset{k_1\ (-\mathrm{H}_2)}{\rightleftharpoons}} \mathrm{X}_2 \underset{k_{-2}}{\overset{k_2}{\rightleftharpoons}} 2\,\mathrm{X}_3 \xrightarrow{k_3\ (+\mathrm{H}_2)} \mathrm{X}_4 \tag{1}$$

Assuming the validity of the mass action law, [5], a system of ordinary differential equations for the time evolution of the concentration of the chemical species X_j, $j = 1, \ldots, 5$, can be derived from the scheme 1 and takes the form:

$$\begin{aligned}
\frac{dX_1}{dt} &= -(k_0 + k_1)X_1 + k_{-1}H_2X_2 \\
\frac{dX_2}{dt} &= k_1X_1 - k_{-1}H_2X_2 + k_{-2}X_3^2 - k_2X_2 \\
\frac{dX_3}{dt} &= k_2X_2 - k_{-2}X_3^2 - k_3H_2X_3^2 \\
\frac{dX_4}{dt} &= k_3H_2X_3^2 \\
\frac{dX_5}{dt} &= k_0X_1
\end{aligned} \tag{2}$$

where we use the notation X_j to also denote the concentrations of the molecule $\mathrm{X_j}$

We now present some basic properties of the model together with a brief description on how the parameters were estimated.

3.2.1 Basic assumptions

To investigate the kinetic model (2) we will assumed that the pressure of hydrogen and the catalyst's concentration are nonzero constants [12]

Aditionally, we will consider that at the initial time $t = 0$ the concentration of all other species except for glycerol (and hydrogen) are zero, i.e.,

$$(X_1, X_2, X_3, X_4, X_5)(0) = (X_1(0), 0, 0, 0, 0) \tag{3}$$

where $X_1(0) > 0$.

3.2.2 Parameters

The rate constants of the model were determined using experimental data from the report of Shozi et al. [13] and then compared using parameters in the report of [7]. In determining the rate constants, first the turnover frequency (TOF) of the catalyst was determined with

guidance from the report of Zhao et al. [18] and then using Arrhenius plots, the order of the reaction was investigated by plotting the logarithm of TOF versus the inverse of temperature.

Reports for these plots with different catalysts used have linear plots and this shows that the reaction is first order [10]. Hence assuming the validity of the mass action law, a plot of the logarithm of glycerol concentration against time is obtained. The slope of this plot is the estimate of the rate constant. In Table 2 below we present their orders of magnitude.

Table 2. Orders of magnitude for the reaction constants obtained using experimental data.

Parameter	Experimental value
k_0	$\leq 10^{-1}$
k_1	$\leq 10^{1}$
k_{-1}	$\leq 10^{1}$
k_2	$\leq 10^{3}$
k_{-2}	$\leq 10^{3}$
k_3	$\leq 10^{3}$

Having looked at the reaction scheme, at the experimental results, and having derived the mathematical model, in the next section we use some techniques from the qualitative theory of ODEs to analyse it.

4 Mathematical analysis

In this section we present some mathematical analysis of the model, mainly its equilibria, properties of the solutions and their stabilities.

4.1 Existence, uniqueness, and boundedness of solutions

It is clear that initial value problems for Equation (2) have unique solutions: the rigt-hand side of (2) is a polynomial vector field. Hence it is C^∞ and, in particular, locally Lipschitz. As a consequence, Picard-Lindelöf theorem guarantees the existence and uniqueness of local solutions to Cauchy problems (see, e.g., Barreira and Valls [1]). In fact, it is easy to see that all nonnegative solutions of (2) are globally defined in $[0, +\infty)$, as shown next:

Proposition 1 *Solutions to* (2) *with nonnegative initial data* $(X_j(0))$ *are nonegative, bounded, and globally defined in a maximal interval containing* $[0, +\infty)$.

Proof. The nonnegativity result is an easy consequence of the structure of (2): since for every $j = 1, \ldots, 5$ at every point of the coordinate half-hyperplanes $\{X_j = 0 \wedge X_i \geq 0 \text{ for } i \neq j\}$ we have $\frac{dX_j}{dt} \geq 0$, and hence $X_j(t) \geq 0$ for $t > 0$. Denote by $\mathbb{R}^{5+}$ the nonnegative cone of $\mathbb{R}^5$. It is also clear from (2) that

$$\frac{d}{dt} \sum_{k=1}^{5} X_k(t) = 0, \tag{4}$$

and thus, for all initial conditions in $\mathbb{R}^{5+}$ it follows that $\sum_{k=1}^{5} X_k(t) = \sum_{k=1}^{5} X_k(0) = C_0$, where C_0 is the constant for each initial condition. Therefore, by the nonnegativity of solutions, $0 \leq X_k(t) \leq C_0$ for all $t \geq 0$ and all $k = 1, \ldots, 5$. From this boundeness result and the fact that the vector field of (2) is polynomial (and hence bounded in bounded sets) it immediately follows that local nonnegative solutions can be extended to a maximal interval containing $[0, +\infty)$. This concludes the proof. ∎

4.2 Equilibria

Proposition 2 *The kinetic model defined by* (2)–(3) *has nonnegative equilibria which are given by*

$$(X_1^*, X_2^*, X_3^*, X_4^*, X_5^*) = (0, 0, 0, (X_4)_{eq}, (X_5)_{eq}), \tag{5}$$

where $(X_4)_{eq} + (X_5)_{eq} = X_1(0)$.

Proof. From the forth and fifth equation in (2) it follows that every equilibria must satisfy $X_1 = 0$ and $X_3 = 0$. Using the first of these conditions in the first equation of (2) we conclude that equilibria must also satisfy $X_2 = 0$. The remaining equations of (2), i.e., the second and third equations, do not provide any other aditional condition, so the remaining two components of the equilibrium solution vector, namely X_4 and X_5, remain free. This proves (5). The relation $(X_4)_{eq} + (X_5)_{eq} = X_1(0)$ follows immediately from (4) and (3). Hence, the equilibria of (2) forms a 2-dimensional plane in the 4-dimensional simplex $\sum_{k=1}^{5} X_k = C_0$ in the positive cone $\mathbb{R}^{5+}$ of the phase plane. ∎

4.3 On the stability of equilibria

4.3.1 Stability of the linearized system

We start the study of the stability of equilibria of (2) by analysing the linearized stability, i.e., the eigenvalues of the jacobian matrix of the right-hand side of (2) about an equilibrium: rewriting equation (2) in vector form gives

$$\mathbf{X}' = \mathbf{F}(\mathbf{X}) \tag{6}$$

where $\mathbf{X}' = (X_1, \ldots, X_5)^\mathsf{T}$ and $\mathbf{F}(\mathbf{X}) = \begin{bmatrix} (-k_0 - k_1)X_1 + k_{-1}H_2X_2 \\ k_1X_1 - (k_2 + k_{-1}H_2)X_2 + k_{-2}X_3^2 \\ k_2X_2 - (k_{-2} + k_3H_2)X_3^2 \\ k_3H_2X_3^2 \\ k_0X_1 \end{bmatrix}$. Hence, the jacobian $D\mathbf{F}(\mathbf{X})$ at a point $\mathbf{X}$ is

$$D\mathbf{F}(\mathbf{X}) = \begin{bmatrix} -k_0 - k_1 & k_{-1}H_2 & 0 & 0 & 0 \\ k_1 & -k_2 - k_{-1}H_2 & 2k_{-2}X_3 & 0 & 0 \\ 0 & k_2 & -2k_{-2}X_3 - 2k_3H_2X_3 & 0 & 0 \\ 0 & 0 & 2k_3H_2X_3 & 0 & 0 \\ k_0 & 0 & 0 & 0 & 0 \end{bmatrix}. \tag{7}$$

Taking $\mathbf{X} = \mathbf{X}_{eq}$ given by (5) we have

$$D\mathbf{F}(\mathbf{X}_{eq}) = \begin{bmatrix} -k_0 - k_1 & k_{-1}H_2 & 0 & 0 & 0 \\ k_1 & -k_{-1}H_2 - k_2 & 0 & 0 & 0 \\ 0 & k_2 & 0 & 0 & 0 \\ 0 & 0 & 0 & 0 & 0 \\ k_0 & 0 & 0 & 0 & 0 \end{bmatrix}.$$

It is easy to compute the characteristic polynomial of this matrix, obtaining

$$\Big(\lambda^2 + (k_0 + k_1 + k_2 + k_{-1}H_2)\lambda + (k_0k_2 + k_1k_2 + k_0k_{-1}H_2)\Big)\lambda^3 = 0. \tag{8}$$

Thus, the eigenvalues of the jacobian $D\mathbf{F}(\mathbf{X}_{eq})$ about an equilibrium $\mathbf{X}_{eq}$ are $\lambda_0 = 0$, with algebraic multiplicity equal to 3, and

$$\lambda_\pm = \frac{-(k_0 + k_1 + k_2 + k_{-1}H_2)}{2} \pm \frac{\sqrt{(k_0 + k_1 + k_2 + k_{-1}H_2)^2 - 4(k_0k_2 + k_1k_2 + k_0k_{-1}H_2)}}{2}, \tag{9}$$

each with algebraic multiplicity 1. Clearly, due to the nonnegativity of the kinetic coefficients, we always have $\mathrm{Re}(\lambda_\pm) < 0$. It is also easy to conclude that the geometric multiplicity of $\lambda_0 = 0$ is equal to its algebraic multiplicity, and thus we can conclude (see, e.g. [1, Theorem 3.10]) that the equilibria of the linear system $\mathbf{u}' = D\mathbf{F}(\mathbf{X}_{eq})\mathbf{u}$ are stable. However, since the jacobian $D\mathbf{F}(\mathbf{X}_{eq})$ is not hyperbolic, from this computation we

cannot infer the stability of the equilibria for the nonlinear system (2), as the Grobman-Hartman theorem [1, Theorem 4.7] is not applicable. Even if it were, the result we would obtain would be just local, for initial conditions sufficiently close to the equilibrium under analysis.

To overcome the above problems we will observe that system (2) is a compartmental system and we use known properties of these systems to proceed with our analysis. We start by briefly reviewing this concept.

4.3.2 Exploring the structure of (2) as a compartmental system

Consider the system

$$\mathbf{m}' = \mathbf{F}(\mathbf{m}) + \mathbf{I}, \tag{10}$$

where $\mathbf{m} = \{m_i\}_{i\in\{1,\dots,n\}}$ is the mass vector of the system's components m_i, $\mathbf{F} = \mathbf{F}(\mathbf{m})$, is the transfer matrix (which typically depends on $\mathbf{m}$) and $\mathbf{I}$ is the flow of materials into and out of the system from and to the environment. A compartment is a unit of the system's material that directly mixes with any inflowing material at all times, hence it an homogeneous entity with mass m_i, and the full system is described by the vector $\mathbf{m}$.

Let us consider in Figure 4 the exchange of matter taking place in the ith compartment of a n compartmental system, where m_i represents the mass of the ith compartment, $F_{pq} = F_{pq}(\mathbf{m}) \geq 0$, with $p, q \in \{1, \dots, n\}$, $p \neq q$, is the flow of material from compartment q to compartment p. The inflows and outflows are the flows into and out of the ith compartment respectively.

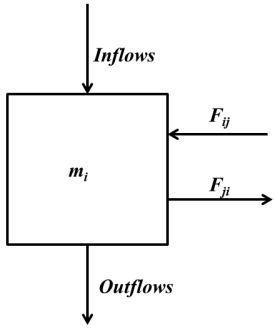

Figure 4. A single compartment of a compartmental system and its flows [6].

We can easily observe that (2) is of the form (10) (with $\mathbf{m} = \mathbf{X}$) with identically zero inflows ($\mathbf{I} = \mathbf{0}$) and outflows. It is also clear from (7) that the right-hand side of the equation (2), $\mathbf{F}(\mathbf{X})$, can be written as $(\mathbf{F}(\mathbf{X}))_{ij} = \sum_{k=1}^{n}(D\mathbf{F}(\mathbf{X}))_{ik}X_k$. Let $f_{ij} = f_{ij}(\mathbf{X}) := (D\mathbf{F}(\mathbf{X}))_{ij}$. Then, we conclude from (7) and from the nonnegativity of the rate coefficients that, in $\mathbb{R}^{5+}$, the ($\mathbf{X}$ dependent) coefficients f_{ij} of the matrix $D\mathbf{F}(\mathbf{X})$ satisfy $f_{ii} < 0, f_{ij} \geq 0$ for $i \neq j$, and $\sum_{i=1}^{n} f_{ij} \leq 0$. This means that, for all $\mathbf{X} \in \mathbb{R}^{5+}$, the jacobian $D\mathbf{F}(\mathbf{X})$ is a compartmental matrix [6].

Now we recall the important result in [6, Theorem 5]:

Proposition 3 *Let $\mathbf{F} = (F_i) : S \to \mathbb{R}^n$ be a C^1 function on an open subset S of $\mathbb{R}^n$. Suppose that for all $\mathbf{X} \in S$ its jacobian $D\mathbf{F}(\mathbf{X})$ is a compartmental matrix. Then:*

1. *the function $G(\mathbf{X}) = \sum_{i=1}^{n}|F_i(\mathbf{X})|$ is a Lyapunov function for (6) (i.e., $t \mapsto G(\mathbf{X}(t))$ is a monotonically nonincreasing function, for every solution $\mathbf{X}(\cdot)$ of (6));*
2. *each orbit of (6) is either unbounded or converges to the set of equilibria when $t \to +\infty$.*

Given the bound (4) on nonnegative solutions to (2) and the conclusion above that, for all $\mathbf{X}$, the jacobian $D\mathbf{F}(\mathbf{X})$ is a compartmental matrix, we conclude that, for all nonnegative initial condition, the positive semi-orbit is nonempty and compact and thus its ω-limit is an equilibrium solution of (2). The determination of exactly which of the equilibria is the ω-limit of the solution starting at a given initial condition $(X_1(0), 0, 0, 0, 0)$ is a difficult problem that does not seem to be completely understood at present. The limit point $\mathbf{X}^*$, which always satisfies

$$X_4^* + X_5^* = X_1(0),$$

depends on the values of k_i, H_2, and $X_1(0)$ as the simulations in the next section illustrates.

5 Results

In this section we present the experimental results as well as simulations from the model. The simulations were done using a programming language called Julia which contains a built in package, *DifferentialEquations.jl* for the simulations and uses the Runge–Kutta fourth-order method. The experimental results were plotted using MS Excel where the

equilibrium concentrations of the products are shown using bar plots. The results are presented at different ratios of hydrogen to glycerol.

5.1 Experimental results

To obtain the results in Figure 5 below, the concentrations of the products were calculated at the end of the reaction.

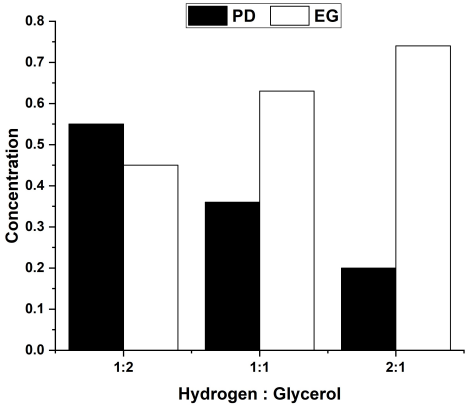

Figure 5. Equilibrium concentrations of EG and PD at different Hydrogen:Glycerol ratios (Shozi et al. [14]). Units for concentration= au

The experimental results showed that when there is more glycerol than hydrogen, the reaction favours the production of PD over EG. However, increasing the amount of hydrogen over that of glycerol results in the production of more EG over .

In the next section we present the simulations from the model in an attempt to compare them with the experimental results. We also present the model results on the limit points for the solutions for each case.

5.2 Model simulations

The simulations were done at 3 different ratios of hydrogen to glycerol and they are presented below. We start by comparing the model simulations using the given parameters in Tables 3, 4, 5 with the experimental results shown in Figure 5.

Hydrogen:Glycerol ratio of 1:2

Figure 6 shows the model simulations when the amount of initial glycerol was two times more than that of hydrogen alongside the actual parameter values used.

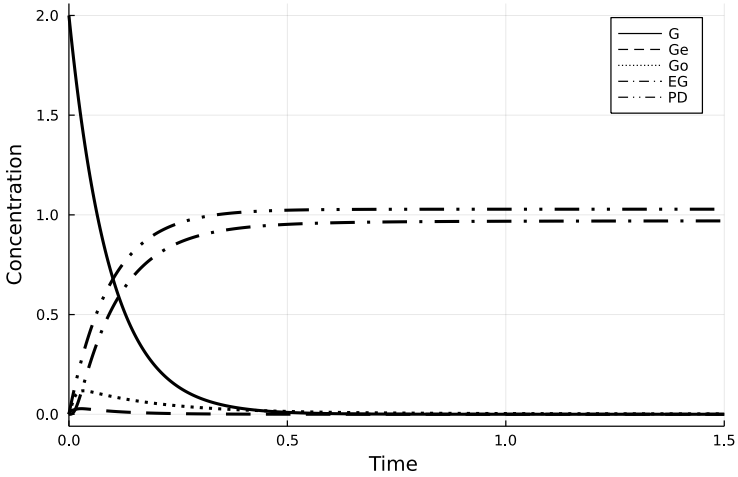

Figure 6. Simulation at Hydrogen:Glycerol ratio of 1:2. Units for concentration= au

Table 3. Corresponding parameter values

Parameter	Value used
k_0	55.0×10^{-1}
$k_1 = k_{-1}$	0.53×10^{1}
$k_2 = k_{-2}$	0.53×10^{3}
k_3	0.53×10^{3}

The simulations from the model showed that when the initial amount of glycerol is more than that of hydrogen, and using the parameters given in Table 3 the reaction favours the production of the PD over the EG, just like what is in the experimental results . Also from the model, we see that the glycerol is converted slowly into the products when the hydrogen is less than the glycerol compared to Figures 7 and 8.

Hydrogen:Glycerol ratio of 1:1

For equal amounts of initial glycerol and hydrogen, the model results obtained are shown in Figure 7 below alongside the parameter values used for the simulation.

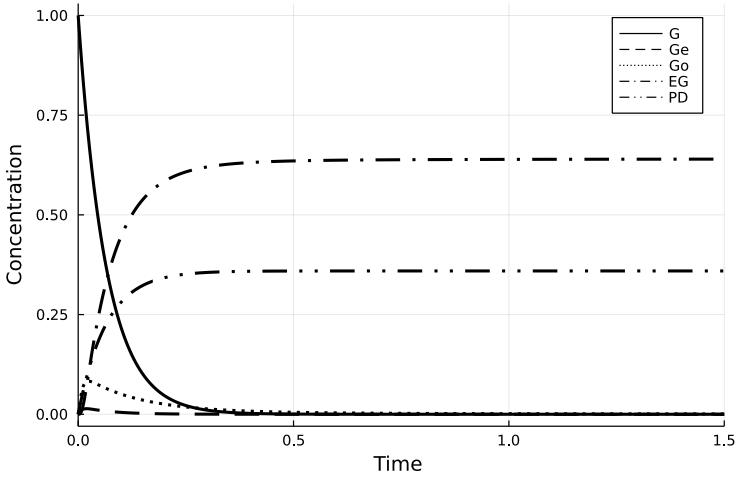

Figure 7. Simulation at Hydrogen:Glycerol ratio of 1:1.
Units for concentration= au

Table 4. Corresponding parameter values

Parameter	Value used
k_0	55.0×10^{-1}
$k_1 = k_{-1}$	1.0×10^{1}
$k_2 = k_{-2}$	1.0×10^{3}
k_3	1.0×10^{3}

When we have equal initial amounts of glycerol and hydrogen, the model predicted that more EG will be produced than PD, a result similar to the one obtained experimentally. At this point, the glycerol is converted into products faster as we can see the curve in Figure 7 for glycerol decays more fast than in Figure 6.

Hydrogen:Glycerol ratio of 2:1

When the hydrogen used was two times more than the initial glycerol, the model simulations obtained were as shown in Figure 8 below along side the parameter values used for the simulation.

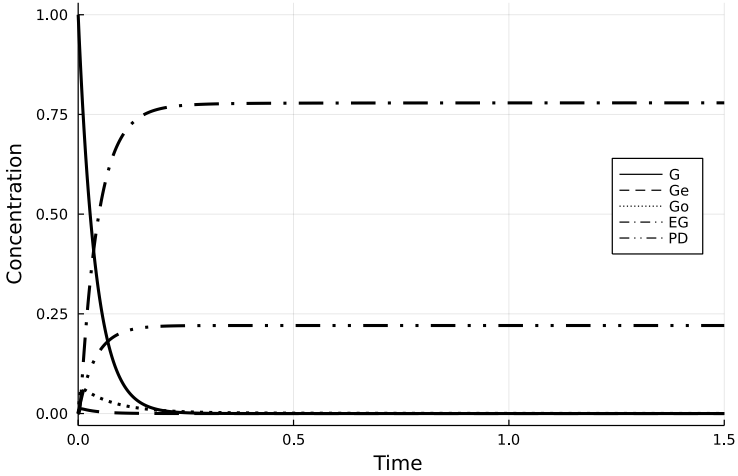

Figure 8. Simulation at Hydrogen:Glycerol ratio of 2:1.
Units for concentration= au

Table 5. Corresponding parameter values

Parameter	Value used
k_0	55.0×10^{-1}
$k_1 = k_{-1}$	2.0×10^{1}
$k_2 = k_{-2}$	2.0×10^{3}
k_3	2.0×10^{3}

The model showed that increasing the amount of hydrogen over that of glycerol still promotes the production of EG over PD as shown by the experimental results. Also, the glycerol is converted into products even much faster than the above two cases.

Having presented the model simulations, we then present the approximations of the limit points for each case as illustrated below.

5.2.1 Limit points

For the different ratios of hydrogen to glycerol the limit points were computed by $X_i^* = \lim_{t\to\infty} X_i(t)$, for $i = 1, \ldots, 5$. These were well approximated by the values of X_i's at large values of t, say t^*, depending on the simulation.

Table 6 below shows the limit points, i.e $(X_1^*, X_2^*, X_3^*, X_4^*, X_5^*)$, from the simulations at the different ratios of hydrogen to glycerol, correct to 2 decimal places.

Table 6. Limit points at different H:G ratios at $t^* = 1.5$

H : G	$X_1(0)$	Limit point	$X_4^* + X_5^*$
1 : 2	2.00	$(0.00, 0.00, 0.00, 0.97, 1.03)$	2.00
1 : 1	1.00	$(0.00, 0.00, 0.00, 0.64, 0.36)$	1.00
2 : 1	1.00	$(0.00, 0.00, 0.00, 0.78, 0.22)$	1.00

Having presented the model simulations and compared them with the experimental results, we then investigate the effects of the constants k_1 and k_{-1} by fixing the the other constants and the ratio of hydrogen to glycerol at 1:1.

Effects of k_1, k_{-1} to the production of EG and 1,2-PD

When the ratio of hydrogen to glycerol was fixed at 1:1 as well as k_0, k_2, k_{-2}, k_3 and only varying k_1 and k_{-1} results were obtained and are given in the following figures.

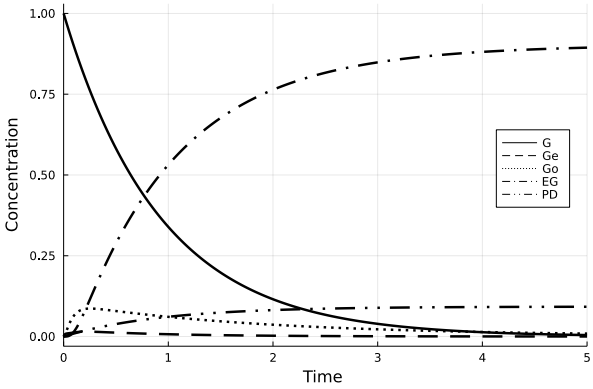

Figure 9. Simulation at Hydrogen:Glycerol ratio of 1:1. Units for concentration= au

Table 7. Corresponding parameter values

Parameter	Value used
k_0	1.0×10^{-1}
$k_1 = k_{-1}$	1.0
$k_2 = k_{-2}$	1.0×10^2
k_3	1.0×10^2

Increasing the value of $k_1 = k_{-1}$ gave the following simulations.

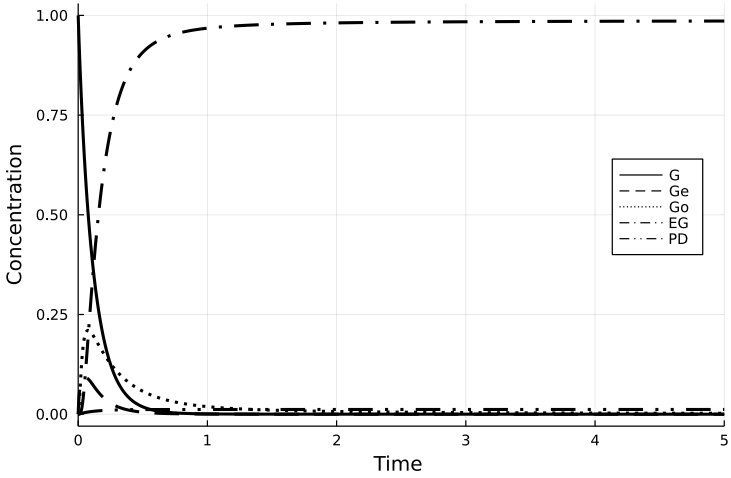

Figure 10. Simulation at Hydrogen:Glycerol ratio of 1:1. Units for concentration= au

Table 8. Corresponding parameter values

Parameter	Value used
k_0	1.0×10^{-1}
$k_1 = k_{-1}$	10.0
$k_2 = k_{-2}$	1.0×10^2
k_3	1.0×10^2

The results show that increasing the values of k_1 and k_{-1} yields to an increase in the amount of EG produced and the reaction reaches equilibrium faster as it seen the the

Figures 9 and 10. Limit points were also approximated like in the above way (see Section 5.2.1) and they are presented in Table 9 below, correct to 2 decimal places.

Table 9. Limit points when varying k_1, k_{-1} and fixing the other parameters at $t^* = 5.0$

Figure	$X_1(0)$	Limit point	$X_4^* + X_5^*$
Fig. 9	1.00	$(0.00, 0.00, 0.00, 0.91, 0.09)$	1.00
Fig. 10	1.00	$(0.00, 0.00, 0.00, 0.99, 0.01)$	1.00

We have presented the findings from the experiment and the model simulations, in the next section we then proceed by presenting the discussion of both the mathematical results and the simulations.

6 Discussion and conclusion

In this section we present the analysis of the mathematical results and model simulations, conclusions as well as future work. We start by presenting the discussion of the results obtained from the mathematical analysis of the model.

6.1 Mathematical results analysis

The kinetic model consists of a 5-dimensional system of autonomous nonlinear ordinary differential equations for the evolution of the concentrations $X_j(t)$, $j = 1, \ldots, 5$ of the chemical species taking part in the chemical reaction scheme. The mathematical investigations of the system showed that, for each nonnegative initial condition, the corresponding solution is unique, defined for all positive times, bounded and lie on 2 dimensional plane in a 4-dimensional simplex. We also concluded that it converges to some limit point as $t \to +\infty$, which may depend on the initial condition. This is so because, due to the above invariance and to the special structure of the vector field defining the model (a system whose jacobian matrix is everywhere a compartmental matrix), each solution has a nonempty ω-limit set which is an equilibrium (by Proposition 3).

We then look at the discussion of the simulations from the model.

6.2 Model simulation analysis

The model and experimental results have almost similar outcomes in all the 3 different ratios of hydrogen to glycerol. From Figure 6 where we have initial glycerol concentration two times more than hydrogen, the model results showed that more PD is produced over EG. This is because, according to [16] the Cu-Re/ZnO catalyst used have acidic sites which favours the removal of a water molecule over that of hydrogen, hence more PD is produced over EG. From Figures 7 and 8, an increase in the hydrogen to glycerol ratio led to an increase in the production of EG over PD.This can be due to the further hydrogenolysis of the PD into EG and other products, as reported in the report by [16].

The model results also showed that an increase in the hydrogen to glycerol ratio resulted in the increase in the conversion of glycerol into the products. This is likely caused by the increase in the catalyst's activity in the presence of hydrogen, which promotes mostly the removal of hydrogen gas from glycerol over the water molecule. Likewise, the results showed that increasing the amount of hydrogen over that of glycerol does not necessarily bring great change in the amount of EG produced since their equilibrium concentrations do not differ much. If increasing the amount of hydrogen does not bring much increase in EG production, it means that the hydrogenolysis process is cost-effective, since the production of hydrogen is very costly [5].

When we fixed the ratio of hydrogen to glycerol at 1:1 as well as the other constants while varying only k_1, k_{-1}, the model simulation showed that an increase in the value of k_1, k_{-1} results in an increase in the production of EG, as shown in Figure 10. This is because, from system (1) we see that an increase in these constants means more glycolaldehyde will be formed which consequently means more glyceraldehyde is produced hence the increase in the EG formed.

At higher k_1, k_{-1}, the reaction reaches equilibrium faster than at lower values as it is shown by Figures 9 and 10. This might be due to that the intermediates are produced at a higher rate and quickly utilized into products as shown by Figure 10, we have more glycolaldehyde produced and quickly levels to 0 compared to Figure 9.

6.3 Conclusion

The reaction for the hydrogenolysis of glycerol can be modelled using a system of ordinary differential equations and the model simulations were aligned with how the reaction proceeds in the chemistry point of view. All solutions of the model converge to some stable limit point in a 2 dimensional plane of a positive cone in the $\mathbb{R}^5$ space, and they depend on the values of k_i and hydrogen to glycerol ratio used. However, finding the exact limit point to which the solutions converge to, is a problem that is not fully understood at the moment, possibly due to the fact that our model is non-linear, hence other mathematical tools needs to be used.

7 Future work

The work reported here is based on a specific chemical mechanism modelling the hydrogenolysis of glycerol published in the literature. Other models have also been proposed in the literature and it would be interesting to study those ones using the tools of mathematical analysis and simulations so that comparison with experimental results can lead to a better understanding of this important complicated catalytic mechanism that is, at present, not thoroughly understood. In fact, it is recognized that even the model studied here needs some revision since the experimental molar ratio of produced ethylene glycol:methanol is about 4:1 and not 1:1 as the kinetic scheme under consideration predicts.

Notwithstanding the concrete model to be considered in the future, the tools used in this work (mathematical analysis based on qualitative analysis tools and simulations supported by numerical solutions of ODE) are bound to be crucial in that process. A deeper understanding might also require other mathematical tools that have not been studied or used here, such as methods from asymptotic analysis, and others.

Acknowledgements: The authors acknowledge the African Institute for Mathematical Sciences (AIMS)-ZA and The MasterCard foundation for funding this work. FPdC was partially supported by FCT/Portugal through CAMGSD, IST-ID , projects UIDB/04459/2020 and UIDP/04459/2020.

References

[1] L. Barreira, C. Valls, *Ordinary Differential Equations: Qualitative Theory*, Am. Math. Soc., Providence, 2012.

[2] J. J. Bozell, G. R. Petersen, Technology development for the production of biobased products from biorefinery carbohydrates — the US department of energy's "top 10" revisited, *Green Chem.* **12** (2010) 539–554.

[3] J. W. Cain, Chemical reaction kinetics: Mathematical underpinnings, in: E. Bell (Ed.), *Molecular Life Sciences*, Springer, New York, 2020.

[4] ENERGY.GOV. US Department of Energy. *Biodiesel Production,* `https://afdc.energy.gov/fuels/biodiesel-production.html`, Accessed April 2019.

[5] M. Feinberg, *Foundations of Chemical Reaction Network Theory*, Springer, Cham, 2019.

[6] J. A. Jacquez, C. P. Simon, Qualitative theory of compartmental systems, *SIAM Rev.* **35** (1993) 43–79.

[7] X. Jin, B. Subramaniam, R. V. Chaudhari, P. S. Thapa, Kinetic modeling of pt/c catalyzed aqueous phase glycerol conversion with in situ formed hydrogen, *AIChE J.* **62** (2016) 1162–1173.

[8] D. G. Lahr, B. H. Shanks, Kinetic analysis of the hydrogenolysis of lower polyhydric alcohols: glycerol to glycols, *Ind. Eng. Chem. Res.* **42** (2003) 5467–5472.

[9] G. M. Lari, G. Pastore, M. Haus, Y. Ding, S. Papadokonstantakis, C. Mondelli, P. Ramírez, Environmental and economical perspectives of a glycerol biorefinery, *Eng. Env. Sci.* **11** (2018) 1012–1029.

[10] S. Mondal, H. Malviya, P. Biswas, Kinetic modelling for the hydrogenolysis of bio-glycerol inthe presence of a highly selective Cu-Ni-Al_2O_3 catalyst in a slurry reactor, *React. Chem. Eng.* **4** (2019) 595-–609.

[11] N. Pandhare, S. M. Pudi, S. Mondal, K. Pareta, M. Kumar, P. Biswas, Development of kinetic model for hydrogenolysis of glycerol over Cu/MgO catalyst in a slurry reactor, *Ind. Eng. Chem. Res.* **57** (2017) 101–110.

[12] R. V. Sharma, P. Kumar, A. K. Dalai, Selective hydrogenolysis of glycerol to propylene glycol by using Cu: Zn: Cr: Zr mixed metal oxides catalyst, *Appl. Catal. A: Gen.* **47** (2014) 147–156.

[13] M. L. Shozi, V. D. Dasireddy, S. Singh, P. Mohlala, D. J. Morgan, H. B. Friedrich, Hydrogenolysis of glycerol to monoalcohols over supported Mo and W catalysts, *ACS Sustainable Chem. Eng.* **4** (2016) 5752–5760.

[14] M. L. Shozi, V. D. Dasireddy, S. Singh, P. Mohlala, D. J. Morgan, S. Iqbal, H. B. Friedrich, An investigation of Cu–Re–ZnO catalysts for the hydrogenolysis of glycerol under continuous flow conditions, *Sustain. Energy Fuels* **1** (2017) 1437–1445.

[15] M. L. Shozi, V. D. Dasireddy, S. Singh, P. Mohlala, A. Govender, S. Iqbal, H. B. Friedrich, The effect of rhenium on the conversion of glycerol to mono-alcohols over nickel catalysts under continuous flow conditions, *Sustain. Energy Fuels* **3** (2019) 2038–2047.

[16] A. Torres, D. Roy, B. Subramaniam, R. V. Chaudhari, Kinetic modeling of aqueous-phase glycerol hydrogenolysis in a batch slurry reactor, *Ind. Eng. Chem. Res.* **49** (2010) 10826–10835.

[17] Y. Wang, J. Zhou, X. Guo, Catalytic hydrogenolysis of glycerol to propanediols: A review, *RSC Adv.* **5** (2015) 74611–74628.

[18] H. Zhao, L. Zheng, X. Li, P. Chen, Z. Hou, Hydrogenolysis of glycerol to 1,2-propanediol over Cu-based catalysts: A short review, *Catal. Today* **355** (2019) 84–95.